Lawrence Berkeley National Laboratory
Recent Work

Title
VORTEX METHODS AND TURBULENT COMBUSTION

Permalink
https://escholarship.org/uc/item/4nd5n8v6

Author
Sethian, J.A.

Publication Date
1984-03-01

Lawrence Berkeley Laboratory

UNIVERSITY OF CALIFORNIA

Physics Division

Mathematics Department

VORTEX METHODS AND TURBULENT COMBUSTION

J.A. Sethian

March 1984

DISCLAIMER

VORTEX METHODS AND TURBULENT COMBUSTION[1]

J.A. Sethian

Department of Mathematics
and
Lawrence Berkeley Laboratory
University of California
Berkeley, California 94720

March 1984

Vortex Methods and Turbulent Combustion [1]

J.A. Sethian [2]

Department of Mathematics

and

Lawrence Berkeley Laboratory

University of California

Berkeley, California 94720

Abstract

We describe a series of numerical experiments using random vortex element techniques coupled to a flame propagation algorithm based on Huyghens principle to model turbulent combustion. We solve the equations of zero Mach number combustion for the problem of a flame propagating in a swirling flow inside a closed vessel. We analyze the competing effects of viscosity, exothermicity, boundary conditions and pressure on the rate of combustion in the vessel.

A particularly challenging problem in the study of turbulent combustion within an internal combustion engine is the interaction between hydrodynamic turbulence and the propagation of a flame. The more reactants reached by the flame, the more energy released and the less unburnt fuel expelled at the end of a stroke. At high Reynolds numbers, turbulent eddies and recirculation zones form which affect the position of the flame and the distribution of unburnt fuel available for combustion. Conversely, exothermic effects along the flame front influence the fluid motion.

As one might expect, the full set of equations that describe the above phenomenon is highly complex; the equations are usually simplified in such a way as to highlight a particular aspect of the combustion process, see [3], [12], [18]. For example, most partial differential equation models of turbulent flow are based on a formulation of the Navier-Stokes equations with respect to a mean state, together with a set of equations to include such components as turbulence velocity and length scales. These model are of varying degrees of sophistication and complexity, ranging from zero-equation models ("mean-field closures") to higher order stress equation models. (For an excellent over-view, see [3],[18]). From the combustion side, starting with Landau's work [11], questions of flame stability have received considerable attention over the past few decades, with much of the analysis concentrating on perturbation analysis of various models of combustion, containing such effects as mixing and flame speed dependence on curvature. An excellent, though now slightly outdated, review of such techniques may be found in [14].

Our work has been concerned with developing numerical methods to analyze the effects of such factors as viscosity, exothermicity, boundary conditions and pressure on the interaction between flame propagation and tur-

bulent eddies. At the foundation of our investigations is the random vortex method [6], a grid-free numerical technique that is specifically designed for high Reynolds number flow and portrays in a natural and effective manner the formation of turbulent eddies and coherent structures. Other applications of this method have included flow past an airfoil [4] and blood flow past heart valves [15]. The random vortex method and the flame propagation algorithm described here were first used in a combustion setting to model turbulent combustion over a backwards facing step in [8]. In this review, we assemble the results of a series of numerical experiments we have designed to analyze some components in turbulent combustion; results described have been presented in [13], [19], [20], [21] and [22].

Statement of Problem/Equations of Motion

We consider two-dimensional, viscous flow inside a closed square. On solid walls, we require that the normal and tangential fluid velocities be zero. Combustion is characterized by a single step irreversible chemical reaction; the fluid is a pre-mixed fuel in which each fluid particle exists in one of two states, burnt and unburnt. When a particle burns, it undergoes an instantaneous increase in volume and becomes burnt. Thus, the flame is viewed as an infinitely thin front acting as a source of specific volume and separating the burnt regions from unburnt regions. We assume that the fluid is initially swirling in a counterclockwise direction and at $t=0$ we ignite the fluid at a point halfway up the left side. Our goal is to analyze the interaction of the swirling fluid with the propagating flame front.

Our model is described by the *equations of zero Mach number combustion*, which hold under the assumption that the Mach number M is small, the initial pressure is spatially uniform within terms of order M^2 and the initial conditions for velocity, pressure and mass fraction are consistent within order M. Under these conditions, asymptotic limits of the full Navier-Stokes plus combustion equations can be taken to yield a set of equations that allow for large heat release, substantial temperature and density variations and interaction with the hydrodynamic flow field, but removes the detailed effects of acoustic waves and instead contains a time-dependent spatially uniform mean pressure term. This model can be viewed as existing "in between" constant density models, in which the fluid mechanics essentially decouples from the hydrodynamics, and the fully compressible combustion equations. The full derivation of this model may be found in [13]; a related model for thermally driven bouyant flows applicable to problems in fire research may be found in [17]. We summarize the equations for zero Mach number combustion below.

Let $\vec{v}$ be the fluid velocity vector and let $\vec{v} = \vec{w} + \nabla\varphi$ be the unique decomposition of $\vec{v}$ into a divergence-free component $\vec{w}$ and a curl-free component $\nabla\varphi$. We take the curl of the zero Mach number momentum equation to produce the

VORTICITY TRANSPORT EQUATION

$$\frac{D\xi}{Dt} = \frac{1}{R}\nabla^2 \xi \qquad (1)$$

where $\xi = \nabla \times \vec{w}$ is the vorticity and $\frac{D}{Dt}$ is the total derivative $\partial_t + (\vec{v} \cdot \nabla)$. Here, we have ignored the term $(\nabla \times \frac{\nabla P}{\rho})$ which corresponds to vorticity production across the flame front (We hope to assess the importance of this term at a

later date). The boundary conditions are that $\vec{v} = 0$ on the boundary of the domain.

We view the flame front as a curve separating the burnt and unburnt regions. Let $\vec{r}(t)$ be a point on the front. The front burns normal to itself with speed k and is advected by the flow yielding the

EIKONAL EQUATION FOR THE FLAME FRONT

$$\frac{d\vec{r}}{dt} = k \cdot \vec{n}(\vec{r}) + \vec{v}_u(\vec{r}) \tag{2}$$

where $\vec{v}_u$ is the fluid velocity on the unburnt side, $\vec{n}$ is the unit normal to the front at $\vec{r}(t)$ and the burning speed k is determined from the mass flux m across the flame front by

$$k = \frac{m(\rho_u(t), P(t))}{\rho_u(t)} \tag{3}$$

Here, ρ_u is the density of the unburnt fluid and P is the mean pressure. The rise in presure, which results from fluid expansion along the front, depends on the length of the front and the volume of the vessel and is given by the

NON-LINEAR O.D.E. FOR THE MEAN PRESSURE $P(t)$

$$\frac{dP}{dt} = \frac{q_0 \gamma m}{Vol} L \tag{4}$$

where q_0 is the non-dimensional heat release, Vol is the volume of the vessel and L is the length of the flame front. We assume a γ-gas law and take the mass flux to be of the form

$$m(\rho_u, P) = Q \rho_u^{\frac{1}{2}} P^{\frac{1}{2}} \tag{5}$$

where Q is the local laminar flame velocity, see [3]; ρ_u may then be obtained from the pressure through the relation

$$\rho_u = (P(t))^{1/\gamma} \rho_u(0))$$ (6)

where $\rho_u(0)$ is the density of the unburnt fluid initially. Finally, the Neumann compatibility condition yields the

ELLIPTIC EQUATION FOR THE EXOTHERMIC VELOCITY FIELD $\nabla \varphi$

$$\nabla^2 \varphi = \frac{1}{\gamma P}\left(-\frac{dP}{dt} + q_0\, \gamma\, m\, \delta_F\right)$$ (7)

where δ_F is the surface Dirac measure concentrated on the flame front. Equations (1-7) form our equations of motion.

Numerical Algorithm

Faced with the above set of equations, a standard method would be to employ finite difference techniques to produce a discrete approximation to all of the derivatives and then solve the resulting set of algebraic equations. When applied to the turbulence part of combustion models, some of the problems inherent in such techniques are   1) the necessity of a fine grid in the boundary layer region near walls where sharp gradients exist   2) the introduction of numerical diffusion; the error associated with the approximation equations looks like a diffusion term and hence places a computational upper bound on the size of the Reynolds number that can be effectively modelled and 3) the intrinsic smoothing of finite difference schemes which damps out physical instabilities. The random vortex method, introduced in [6] is a grid-free approximation to the equations of viscous flow at high Reynolds number that

avoids the introduction of mean states and turbulence closure relations and concentrates on following the motion of vorticity by means of a collection of vorticity approximation elements. This technique avoids the averaging and smoothing associated with finite difference formulations and allows us to follow the development of large-scale coherent structures in the flow.

When one considers finite difference approximations to the equation for flame propagation (Equation 2), a typical method is to place marker particles along the boundary of the burnt region and formulate a set of ordinary differential equations corresponding to the motion of these marker particles. At each time step, interpolation through these markers provides an approximation to the position of the flame front. There are some problems involved with such an algorithm. It is difficult to accurately determine the normal direction (needed in Equation 2) from such an algorithm and hence the numerical approximation to the propagating front usually becomes unstable and develops oscillations. Furthermore, it has been shown (see [19]) that the propagating front can develop cusps, analogous to shocks, where the front ceases to be differentiable and the normal is no longer defined. The technique of adding and subtracting marker particles as the front moves requires initial assumptions about differentiability and bounds on curvature. Another problem associated with marker techniques is a topological one; when two burnt regions burn into each other, such a method must "decide" how and which markers are connected and eliminate those no longer on the boundary of the flame. The numerical technique we use is based on a "volume" fraction algorithm; the technique does not require a determination of the normal direction and is not subject to the topological issue mentioned above.

Our technique will be to keep track of the vorticity as a way of computing $\vec{w}$ and to keep track of the flame front as a way of computing $\nabla\varphi$; combining these two at any time will yield the full velocity $\vec{v} = \vec{w} + \nabla\varphi$. We divide the square D into two regions; an interior region where we solve the full vorticity transport equation together with the boundary condition $\vec{v} \cdot \vec{n} = 0$ on ∂D (normal component vanishes) and a boundary layer region where we solve the Prandtl boundary layer equations together with the boundary condition $\vec{v} \equiv 0$ on ∂D (no-slip). In both regions, we use the technique of operator splitting to first update the vorticity with respect to the advection term and then with respect to the diffusion term. Similarly, we update the flame position by first allowing it to burn normal to itself and then by advecting the flame by the hydrodynamic flow field, calculating the exothermic velocity field $\nabla\varphi$ from the elliptic equation (Equation 7). Finally, we solve the non-linear ordinary differential equation to compute the resulting rise in pressure. The separate components are as follows.

Computation of w

We update ξ (Equation 1) where $\xi = \nabla \times \vec{w}$ by following the motion of vorticity through the use of vortex "blobs" as introduced by Chorin in [6]. Knowledge of the position of these blobs at any time provides w. We briefly describe the method; for details, see [6], [8], [21].

We have the vorticity advection equation $\partial_t \xi = -(\vec{w} \cdot \nabla)\xi$. Since $\nabla \cdot \vec{w} = 0$, there exists a stream function ψ such that $\vec{w} = (\psi_y, -\psi_x)$ and $\xi = -\nabla^2\psi$. We may write velocity as a function of vorticity through the fundamental solution to the Laplacian, namely

$$\psi(\bar{x},t) = \int G(\bar{x} - \bar{x}') \, \xi(\bar{x}',t) \, d\bar{x}'$$

where

$$G(\bar{x} - \bar{x}') = \frac{1}{2\pi} \log |\bar{x} - \bar{x}'|$$

and $\bar{x} = (x,y)$. Hence

$$\textit{\^{v}} = \int K(\bar{x} - \bar{x}') \xi(\bar{x}',t) \, d\bar{x}' \tag{9}$$

where

$$K(\bar{x} - \bar{x}') = \frac{(-y,x)}{2\pi |\bar{x} - \bar{x}'|}$$

Let $\bar{x}(t)$ be the position of a particle moving in a fluid at time t. Since vorticity is advected by its own velocity field, we have that $\xi(\bar{x}(t)) = \xi(\bar{x}(0))$, that is, each particle "carries" its own vorticity with it. Our technique will be to exploit this fact; we place N of particles in the flow at $t=0$ and follow their motion. At any later time we have a distribution of these "delta functions" of vorticity which can be "smoothed out" to allow one to compute the resulting velocity field $\textit{\^{v}}$ through Equation (9) (Alternatively, one can view this smoothing process as something that happens to the kernel K). There are two obvious numerical parameters involved in the above; the number N of vortex "blobs" use to describe the initial vorticity distribution and the smoothing factor σ used to compute the velocity field. We use the smoothing structure introduced in [6]; consider N vortex "blobs" placed on an initial grid in the domain, each with "smoothed" stream function

$$\psi(\bar{x}) = \begin{cases} -\dfrac{k_i}{2\pi} \log |\bar{x}| & r \geq \sigma \\[2ex] -\dfrac{k_i}{2\pi} (|\bar{x}| / \sigma + \log |\bar{x}| - 1) & r < \sigma \end{cases}$$

where k_i is the strength (vorticity) of the ith vortex blob. To go from one time step to the next, we use the positions of the vortex blobs to determine the velocity field from Equation (9) and numerically update these positions using Heun's method. Convergence of the vortex method was first established in [9]; for work relating to theoretical aspects of this method, see [1], [2], [9] and [10]. To satisfy the normal boundary condition $\vec{w}\cdot\vec{n} = 0$, we add a potential flow to the above motion (which, of course, adds no vorticity).

To update the vorticity with respect to the diffusion term $\frac{1}{R}\nabla^2\xi$, after the advection step we allow the vortex elements to undergo a random step, drawn from a Gaussian distribution with mean zero, variance $\frac{2\Delta t}{R}$. Since the random walk constitutes a solution to the diffusion equation, the combined motion of the vortex elements approximates the solution to the full vorticity transport equation (1). For details, see [6], [21].

In the boundary layer, we employ similar techniques, only here our vortex elements are discrete, finite length "sheets" of vorticity. Once again, we use operator splitting to separate the Prandtl boundary layer equations into 1) an advection equation

$$\partial_\xi = -(\vec{w}\cdot\nabla)\,\xi$$

$$\xi = -\partial_y w_x$$

$$\nabla\cdot\vec{w} = 0 \qquad \text{on } \partial D$$

$$\vec{w}(x,y = \infty) = W_\infty(x)$$

where $\vec{w} = (w_x, w_y)$ and W_∞ is the velocity as seen at infinity from the solid wall (the equations are written with respect to a solid wall lying on the x axis)

and   2) a diffusion equation

$$\partial_t \xi = \frac{1}{R} \partial_y^2 \xi$$

(note that in this approximation diffusion only takes place in a direction normal to the solid wall). The x component of the velocity (w_x) is written as a function of vorticity and the y component (w_y) is written as a function of w_x through the incompressibility relation. As before, the positions of the vortex elements are used to approximate the vorticity distribution, allowing one to compute the advection field (w_x, w_y). The vortex sheets are advanced under this advection field and allowed to undergo a random walk in the y direction in response to the diffusion term. In addition, newly created vortex sheets are added at solid walls whenever necessary to satisfy the no-slip condition. Information is passed between the interior and the boundary layer in the following manner; the velocity from the vortex blob calculation tangential to the wall is taken as the velocity W_∞ seen at infinity from the boundary layer. Sheets diffuse away from the wall into the interior and become vortex blobs. Conservation of circulation is maintained; during this exchange, when a sheet moves too far from the wall, it becomes a blob with proper strength and vice versa. The velocity field $\vec{u}$ can be obtained at any time from the positions of the vortex elements; for details, see [7], [21].

Computation of Flame Motion and $\nabla \varphi$

We keep track of the position of the flame by introducing a square grid ij on the domain and assigning each cell a number f_{ij} between 0 and 1 (a "volume fraction", see [16]) corresponding to the amount of burnt fluid in that cell at any given time. The algorithm advances the front in a given direction by drawing in each cell for which $0 \le f_{ij} \le 1$ an interface which represents the

boundary between the burnt and unburnt fluid and moving that interface to provide a new set of volume fractions. The orientation of the interface depends on the value of f_{ij} in both the cell and its neighbors; at any time step, the position of the flame front can be reconstructed from the field of volume fractions. The position of the flame is advanced in response to burning and advection. Burning is accomplished by allowing each cell to ignite all of its neighbors at the prescribed rate k determined from Equation (3); this is an approximation based on Huyghens principle which states that the envelope of all disks centered at the front corresponds to the front displaced in a direction normal to itself, see [5]. In fact, it can be shown that this algorithm capitalizes on the geometric nature of flame propagation described in [19]. After the burning is accomplished, the exothermic velocity field $\nabla\varphi$ is determined (Equation 7) and the full velocity field $\vec{v} = \vec{w} + \nabla\varphi$ is used to advect the flame (as well as the vortex elements). Finally, the pressure is updated according to Equation (5).

Results

We have performed a series of numerical experiments to analyze the various factors described in Equations (1-7). In all of the cases described below, we shall consider a square vessel with sides of length 1m. When the initial condition is a counterclockwise swirl, this will be produced by a vortex placed in the center of the square of sufficient strength so that the velocity tangential to any wall at its midpoint is 1m/s. The initial conditions $P(0) = 1$ and $\rho_u(0) = 1$ were taken, and for viscous calculations we assumed a Reynolds number of 1000. The calculation in [8] for turbulent flow behind a step assumed a propane-air mixture with a laminar burning velocity of 12cm/s and an inlet velocity of 6m/s; this inlet velocity was taken as a characteristic

speed scale to provide a non-dimensional laminar flame speed of $Q = .02$ for a flow of unit inlet speed. Since the velocity induced by our initial vortex increases as we approach the center, it is not clear what to choose as a characteristic velocity. In [21], we took a non-dimensional laminar flame speed of $Q = .14$, corresponding to a characteristic velocity 7 times that of the tangential boundary velocity; in the below results, this characteristic velocity will be used in conjunction with Q. Details about the numerical parameters used in the below calculations may be found in [20], [21] and [22].

Hydrodynamics: Inviscid/Viscous

In Figure 1, we show the results of a hydrodynamics calculation (no flame) comparing inviscid flow to viscous flow. Results are displayed on a 30×30 grid placed in the flow, where the magnitude of the vector at each point denotes the relative speed of the flow. Figure 1A, which is the initial flow, remains unchanged for all time in the inviscid case; the sole vortex remains at the center and the normal boundary condition is satisfied through the potential flow. In the viscous calculation (Figs. 1A-1F), small counterrotating eddies grow in each corner in response to the no-slip boundary conditions. These eddies grow, break away and diffuse downstream, and are replaced by a new set.
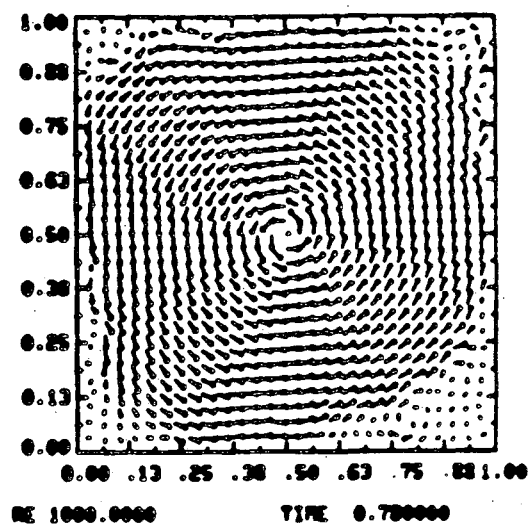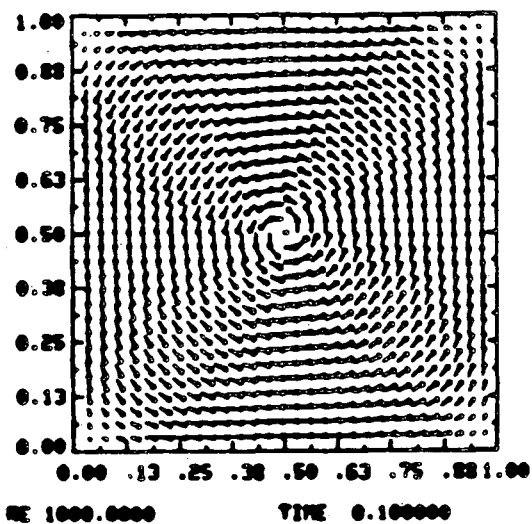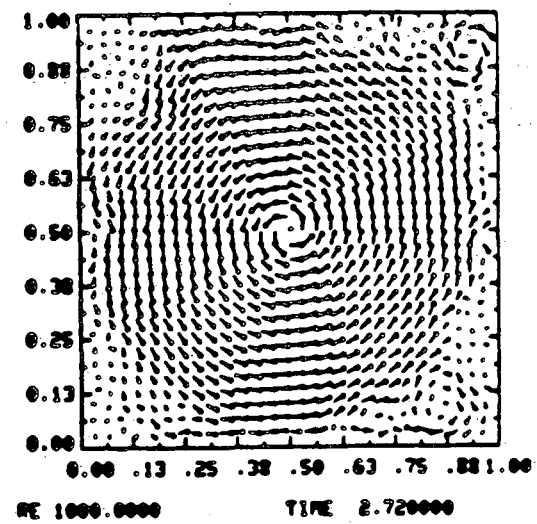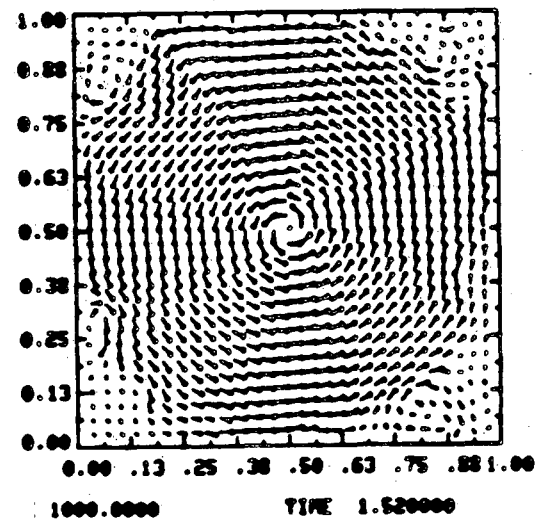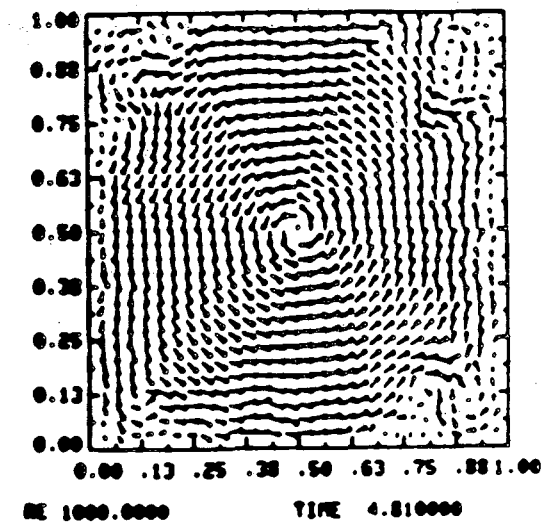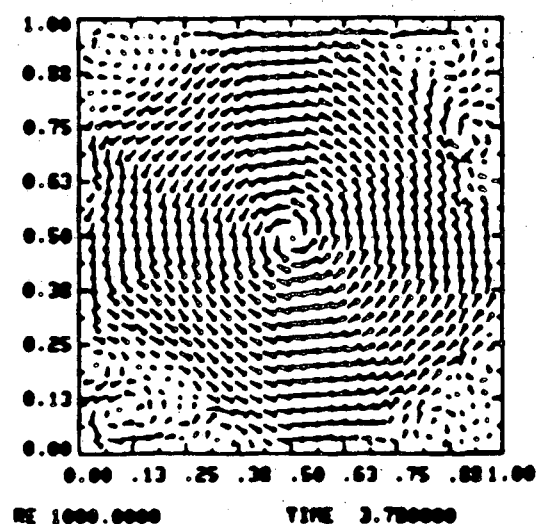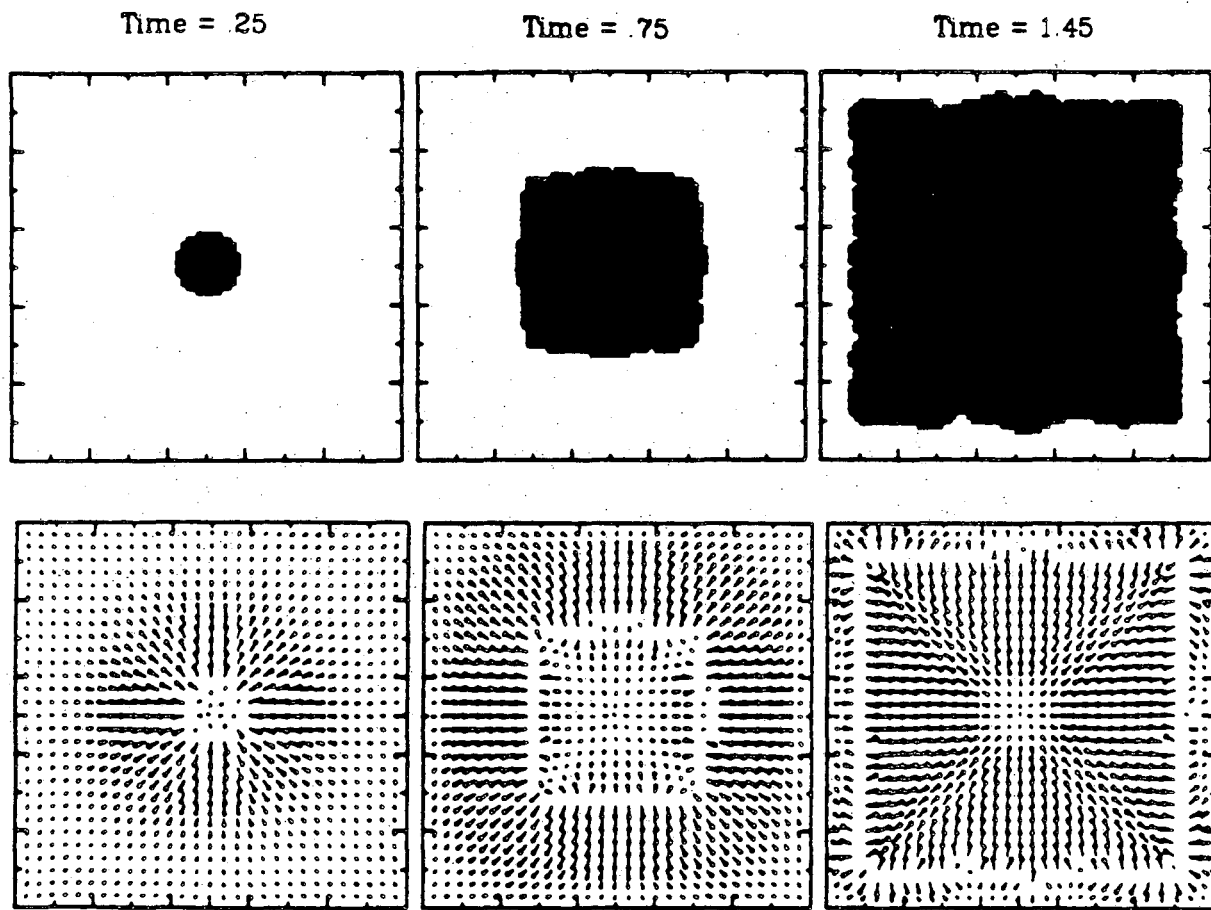
FIGURE 1

Flame Propagation: Pressure and the Exothermic Velocity Field

In the next experiment, a motionless, inviscid fluid is ignited at the center of a closed square. We take a local laminar flame speed $Q=.2$. If the density of the burnt gas is the same as that of the unburnt gas, then the non-dimensional heat release is zero ($q_o = 0$), the pressure remains constant ($\frac{dP}{dt} = 0$ in Equation 4) and the exothermic velocity field $\nabla\varphi$ is identically zero. In this case, the fluid remains still and the flame front is an expanding circle with origin at the center of the square. On the other hand, with $q_o \neq 0$, fluid motion is induced by the propagating flame. In Figure 2, we show results in which $q_o = 1.3333$; this corresponds to an initial ratio of burnt/unburnt of five to one (Here, we assumed an inviscid fluid, hence the no-slip condition is violated). The black region corresponds to the burnt region and once again the velocity is displayed on a 30×30 grid. One can clearly see the mechanism by which the boundary shapes the front; although the front starts off circular, it soon becomes square-like in response to the boundary conditions on $\nabla\varphi$ and thus "burns" into the corners. When the volume was completely burnt, the pressure in the vessel is 2.93 and $k = .24$ (as compared with $k = .2$ at $t = 0$).

Time = .25   Time = .75   Time = 1.45

Inviscid. Motionless Fluid Ignited in Center. $q_0 = 1.333$
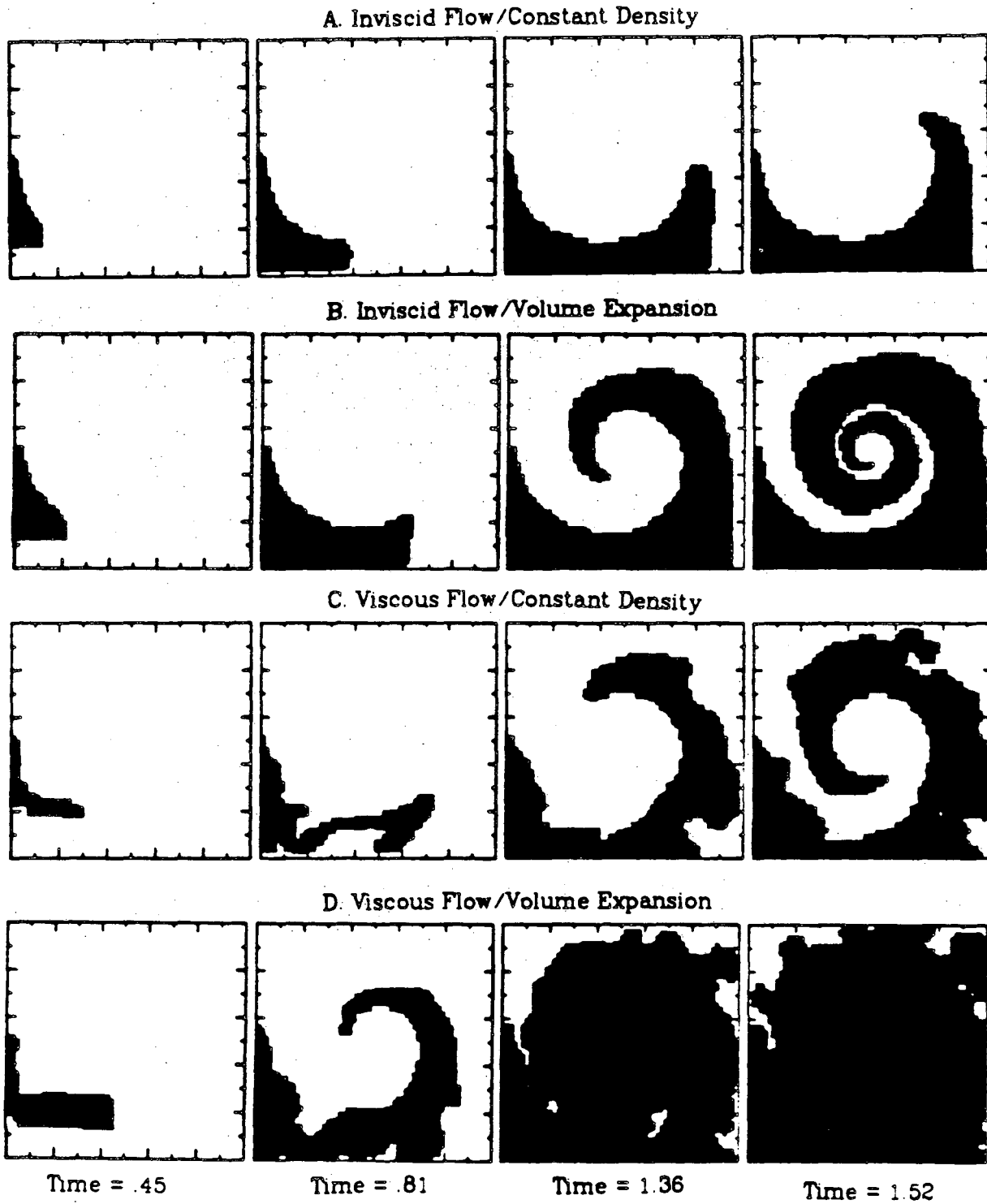
FIGURE 2

Hydrodynamics + Combustion : Exothermicity and Viscosity

Next, we analyze the relative effects of viscosity and exothermicity on the flame motion. Four different experiments were performed with $Q = .14$:

A. Inviscid flow with $q_0 = 0$ (Inviscid/Constant Density),

B. Inviscid flow with $q_0 = 1.3333$ (Inviscid/Volume Expansion),

C. Viscous flow with $q_0 = 0$ (Viscous/Constant Density)

D. Viscous flow with $q_0 = 1.3333$ (Viscous/Volume Expansion).

In the two viscous runs, the flow was started two seconds before ignition so that recirculation zones would have time to develop. The results are show in Figure 3A-3D. In the inviscid, constant density case, the flame is smoothly advected by the large vortex in the center. In the inviscid, exothermic case, the velocity field produced by volume expansion and the rise in pressure and flame speed cause the flame to spiral in towards the center at a faster rate. In the viscous, constant density case, the flame front is twisted by the eddies that develop in the corners; the flame is carried over the eddies and dragged backwards into the corners. The effect of these eddies is to extend the length of the flame front, bringing it into contact with unburnt fuel and increasing the rate at which the vessel becomes fully burnt. Finally, when both viscous and exothermic effects are combined, the flame is both wrinkled due to the turbulence of the flow (hence increasing the surface area of the flame) and carried by the exothermic field; in addition both the flame speed and pressure increase. The effect of these factors is to greatly decrease the amount of time required for complete conversion of reactants to products. In Figure 4 we plot the amount of volume burned vs. time elapsed since ignition, illustrating the above comments.

A. Inviscid Flow/Constant Density

B. Inviscid Flow/Volume Expansion

C. Viscous Flow/Constant Density

D. Viscous Flow/Volume Expansion

Time = .45   Time = .81   Time = 1.36   Time = 1.52
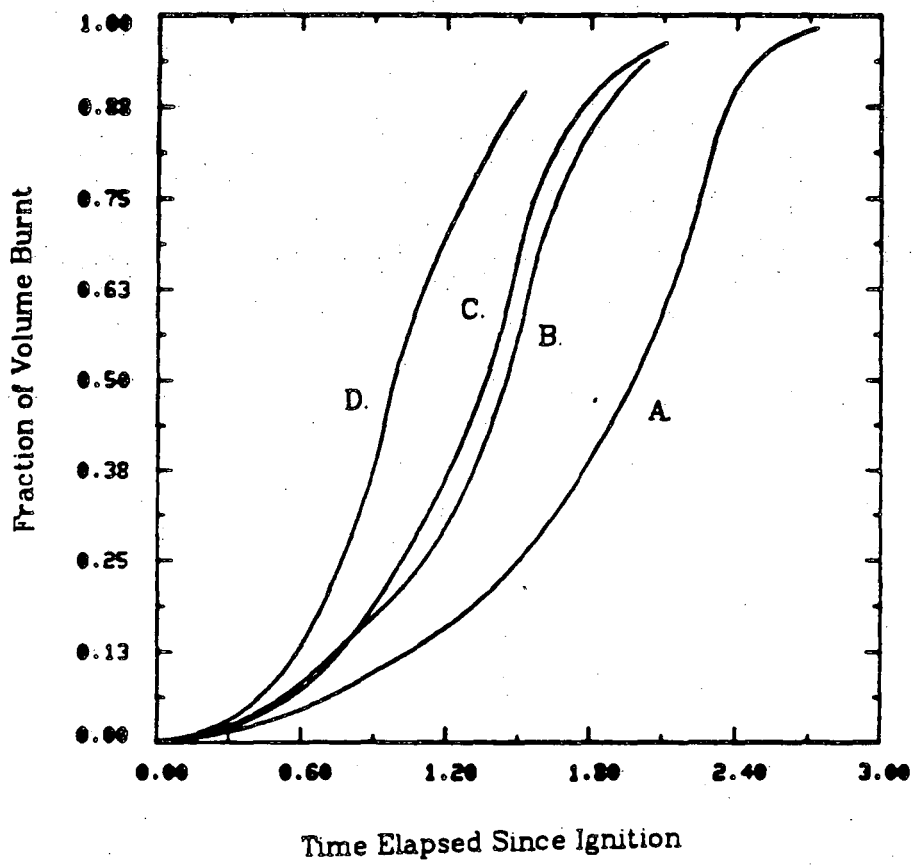
Swirling Fluid

FIGURE 3

FIGURE 4

Flame Wrinkling due to Viscosity as a Function of Laminar Flame Speed

Finally, to further analyze this mechanism of flame wrinkling aue to hydrodynamic turbulence, with Reynolds number 1000 we repeated the viscous, constant density experiment with local laminar flame speed $Q = .02, .06, .1, .14,$ and $.2.$ In Figure 5, we plot the difference in volume burnt between the viscous and the inviscid case against the time elapsed since ignition for each of the above flame speeds. It is obvious that the lower the flame speed the longer the time required for the vessel to becomes completely burnt. However, as the flame speed decreases, viscosity plays an increasingly more important role in the combustion process, as can be seen by noting that the maximum difference between the viscous and inviscid case increases with decreasing flame speed. At low flame speeds, the burning component is overshadowed by the advection component and it is the eddies which are responsible for the lengthing the front and bringing the flame into contact with unburnt fuel. Conversely, when the flame speed is large relative to the advection component, the faster burning rate overshadows this effect and the maximum difference is much less.

As one might expect, the above experiments merely scratch the surface of a highly complicated phenomenon. We are currently investigating such factors as flame speed dependence on curvature, the role of vorticity production along the flame front and the effect of temperature, with the hope of continuing the type of investigation discussed here.
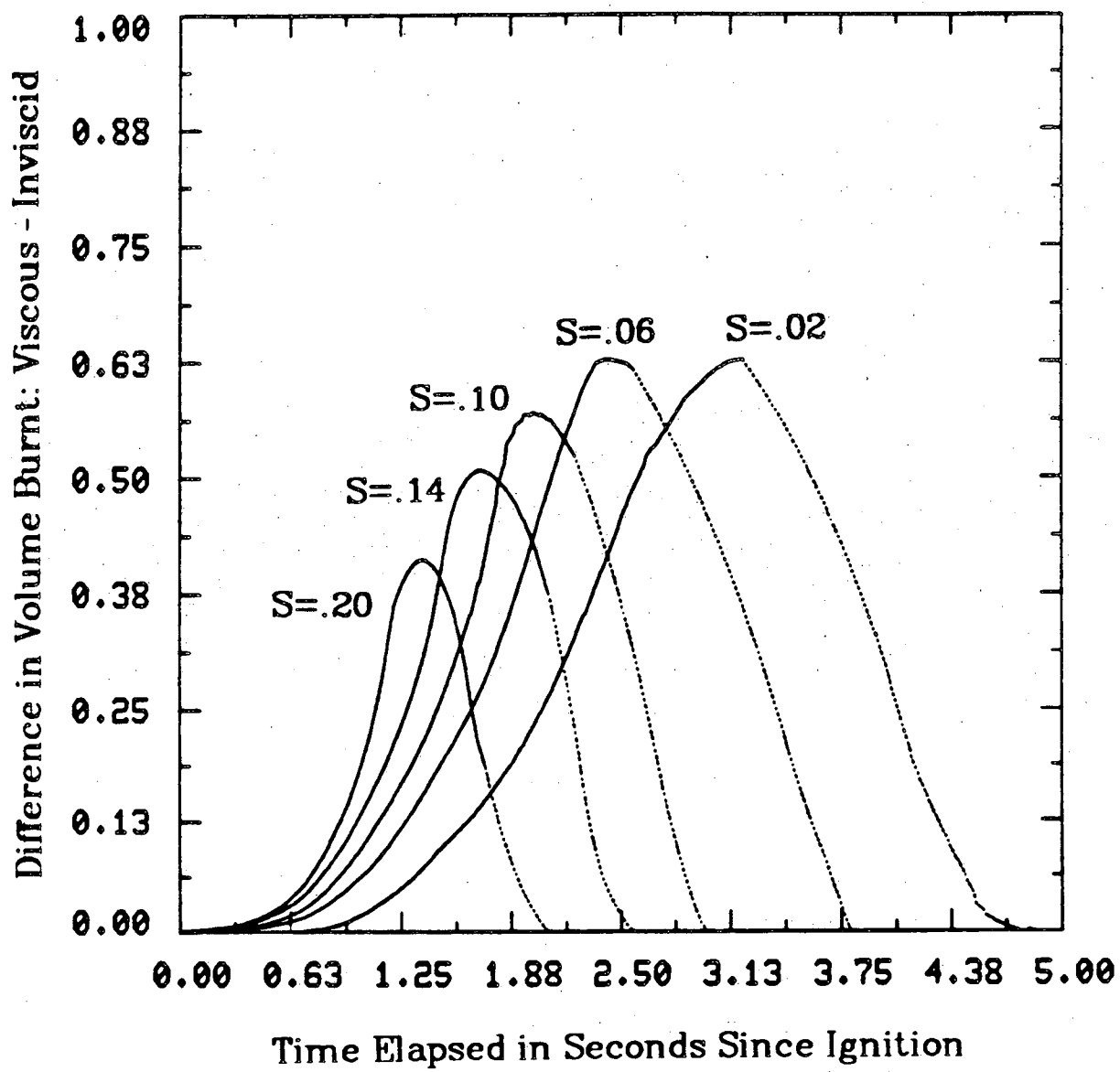
FIGURE 5

REFERENCES

[1] J.T. Beale and A. Majda, *Vortex Methods I; Convergence in Three Dimensions*, Mathematics of Computation, 39 (1982), 1-27.

[2] J.T. Beale and A. Majda, *Vortex Methods II: Higher Order Accuracy in Two and Three Dimensions*, Mathematics of Computation, 39 (1982), 29-52.

[3] K.N.C. Bray, Turbulent Flows with Premixed Reactants, in *Turbulent Reacting Flows* (P.A. Libby and F.A. Williams, ed.), Chap. 5, Springer-Verlag, New York, 1980.

[4] A.Y. Cheer, *A Study of Incompressible 2-D Vortex Flow Past A Circular Cylinder*, SIAM Journal Scientific and Statistical Computation, (1983) 685-705.

[5] A.J. Chorin, *Flame Advection and Propagation Algorithms*, Journal Computational Physics, Vol.35, 1980, 1-11

[6] A.J. Chorin, *Numerical Studies of Slightly Viscous Flow*, Journal of Fluid Mechanics, Vol.57, 1973, 785-796.

[7] A.J. Chorin, *Vortex Sheet Approximation of Boundary Layers*, Journal of Computational Physics, Vol. 27, 1973, 428-442

[8] A.F. Ghoniem, A.J. Chorin, and A.K. Oppenheim, Numerical Modeling of Turbulent Flow in A Combustion Tunnel, Philosophical Transactions of the Royal Society of London, Vol. 304, 1982, 303-325.

[9] O. Hald, *Convergence of Vortex Methods, II* SIAM Journal of Numerical Analysis, 16 (1979),726-755.

[10] O. Hald and V.M. Del Prete, *Convergence of Vortex Methods for Euler's Equations* Mathematics of Computation, 32 (1978), 791-809.

[11] L.D. Landau, *On the Theory of Slow Combustion*, Journal of Experimental Theoretical Physics, 14 (1944), 240-249.

[12] P.A. Libby and F.A. Williams, Fundamental Aspects, in *Turbulent Reacting Flows*, (P.A. Libby and F.A. Williams, ed.), Chap. 1, Springer-Verlag, New York, 1980.

[13] A. Majda and J.A. Sethian, *The Derivation and Numerical Solution of the Equations for Zero Mach Number Combustion*, Lawrence Berkeley Laboratory, LBL-17289, 1984, to appear.

[14] G.H. Markstein, Nonsteady Flame Propagation, Pergammon Press, MacMillan and Company, New York, 1964.

[15] M.F. McCracken and C.S. Peskin, *A Vortex Method For Blood Flow Through Heart Valves*, Journal of Computational Physics, Vol.35, 1980, 183-205.

[16] W.T. Noh and P. Woodward, *SLIC (Simple Line Interface Calculation)*. Proc. 5th Int. Conf. Numer. Math. Fluid Mechanics, Springer-Verlag, Berlin, 1976, 330-339.

[17] R.G. Rehm and H.R. Baum, *The Equations of Motion for Thermally Driven, Bouyant Flows*, Journal of Research of the National Bureau of Standards, Vol. 83, (1978), pp. 297-308

[18] W.C. Reynolds and T. Cebeci, Calculation of Turbulent Flows, in *Turbulence*, (P. Bradshaw, ed.), Chap. 5, Springer-Verlag, Berlin, 1978.

[19] J.A. Sethian, *An Analysis of Flame Propagation*. PhD. Dissertation, University of California, Berkeley, June 1982.

[20] J.A. Sethian, *Numerical Simulation of Flame Propagation in a Closed Vessel*, Proc. Fifth Int. GAMM Conf. Numer. Meth. Fluid Mechanics, Rome, Italy, Oct.5-7, 1983.

[21] J.A. Sethian, *Turbulent Combustion in Open and Closed Vessels*, to appear in the Journal of Computational Physics, June 1984.

[22] J.A. Sethian, *The Wrinkling of a Flame Due to Viscosity*, Fire Dynamics and Heat Transfer, Proc. 21st Nat. Heat Transfer Conf., J.Quintiere, Ed., 29-32, 1983.